Design Proposal: Mach-Zehnder Interferometer

YAMAN PARASHER

[1] *TeCIP Institute, Scuola Superiore Sant'Anna, Pisa, Tuscany, Italy*
[*] *y.parasher@master.sssup.it*

Abstract: This report describes the design, simulation & analysis of a Mach-Zehnder interferometer made with waveguides in the strip configuration alongwith Y-Branch-Splitter & Combiner and bidirectional couplers. Simulated results and analytical evaluations are presented in order to support the design choices. Till now, the first-draft of the layout mask is presented for future fabrication and automated testing processes.

1. Introduction

In the last decades, integrated photonics has significantly contributed for the evolution of the optical communications industry [1], [2]. Namely, silicon photonics devices have shown high-speed/ integration capabilities, associated with improved performance and reduced loss/power consumption. These features have been characterizing silicon photonics as a key element to support the crescent capacity-bandwidth demand of the optical networks. In this context, optical interferometers, as the Mach-Zehnder interferometer (MZI) and the multimode interferometer (MMI), are important devices for the development of, for example, optical modulators, switches and even new-generation reconfigurable optical add-drop multiplexers (ROADMs) [3], [4].

With this motivation, this work is devoted to perform the design, layout and fabrication of MZI/MMI devices using the silicon-on-insulator (SOI) wafer, with strip waveguides [5].This report is organized as follows: Section 2 briefly presents the basic overview of MZI with ways to measure its performance ; Section 3 shows the 3 different layout of the MZI having different values of ΔL; Section 4 concludes the report according to the work done till now.

2. Modeling and Simulations

2.1. Mach-Zehnder Interferometer

The MZI model was constructed in the Lumerical INTERCONNECT software. To perform the light coupling, grating couplers were included in the input/output of the model. A typical unbalanced MZI usually consists of two Y-Branches (a splitter and a combiner) connected by waveguides (upper and lower branches).
In this work, the interference at the MZI output is exploited only by the length mismatch between upper and lower branches. Therefore, both waveguides were modelled for the same cross-section geometry and material properties. Figure 1 presents the schematic used for the modeling. Both waveguides (boxes "Upper-Path" and "Lower-Path") were modelled based on the information exported from the modal analysis. The gratings (boxes "Grating-Coupler-Input" and "Grating-Coupler-Output") and Y-branches (boxes "Y-Branch-Splitter"and "Y-Branch-Combiner") were described based on S-parameters provided in the devices library of this course .Then, simulations for the complete MZI circuit (Figure 1) were performed, for several values of length mismatches in the MZI branches. As expected, the number of oscillations in the transfer function is proportional to the ΔL parameter. Consequently, as predicted by Equation (4), the FSR decreases with the length unbalance.

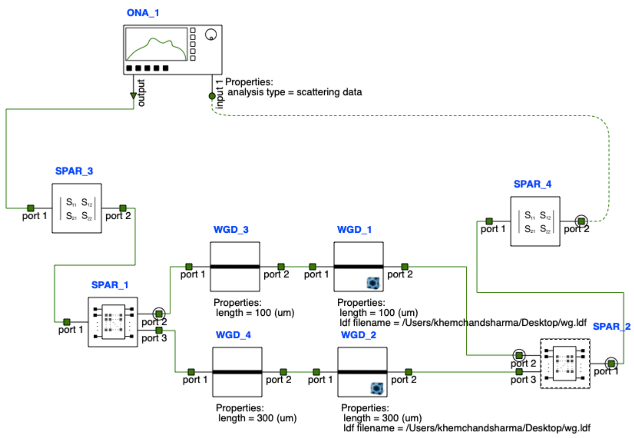

Fig. 1. Proposed MZI model implemented in Lumerical INTERCONNECT.

The transfer function of a MZI can be modeled with the following equation,

$$T = \frac{1}{4}[e^{-}i\beta_1 L_1 + e^{-}i\beta_2 L_2]^2 \tag{1}$$

in which, L_1 and L_2 are the waveguide lengths of the two arms, β_1 and β_2 are the complex propagation constants in the first and the second arm of the MZI. In general, the waveguides can be different, hence the propagation constants are not always the same. The complex propagation constant (β) contains the effects of both dispersion and loss, and is defined as:

$$\beta = \frac{2\pi . n_e(\lambda)}{\lambda} - \frac{i\alpha}{2}. \tag{2}$$

where,

$$n_e(\lambda) = n_1 + n_2(\lambda - \lambda_o) + n_3(\lambda - \lambda_o)^2 \tag{3}$$

where λ is wavelength, n_e is the effective index and α is optical loss. The free spectral range (FSR) which is defined as wavelength spacing between two adjacent peaks is calculated by:

$$FSR = \frac{\lambda^2}{\Delta L . n_g} \tag{4}$$

where ΔL is the path length difference between two arms of MZI, and n_g is the group index.

3. Layout

The design proposal was developed in KLayout software. The draft layout mask is depicted in Figure 2, for three different MZIs geometries. A few details were demanded in design, in order to make possible the future automated testing. While designing the main considered restrictions were the following: first, the TE grating couplers were oriented to the right side, to speed up the tests, avoiding unnecessary chip rotations; second, a 127 μm pitch was fixed, for the input and output gratings, to match with the pitch of the fiber array used in the automated measurements. Besides that, in order to mitigate the bend losses [5], all the TE-devices curves have a radius of 5μm. After simulating each of the three MZI structures layout in Lumerical Interconnect, we get the spectrum defined by Figure 3,4 5 respectively for three different ΔL = 100 , 200, 300μm.

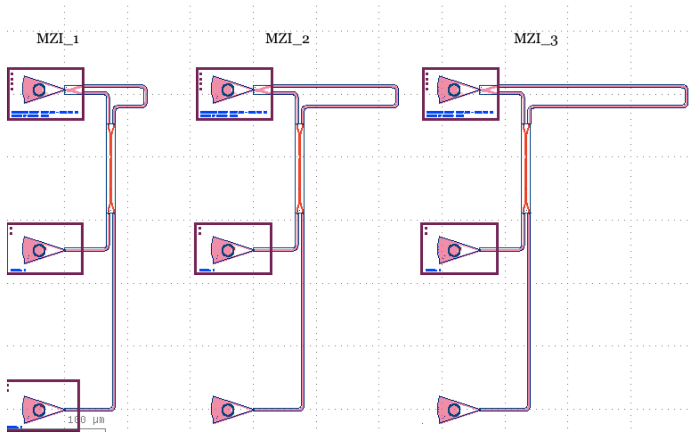

Fig. 2. First version layout of different MZI geometries with ΔL = 100 , 200, 300μm respectively.

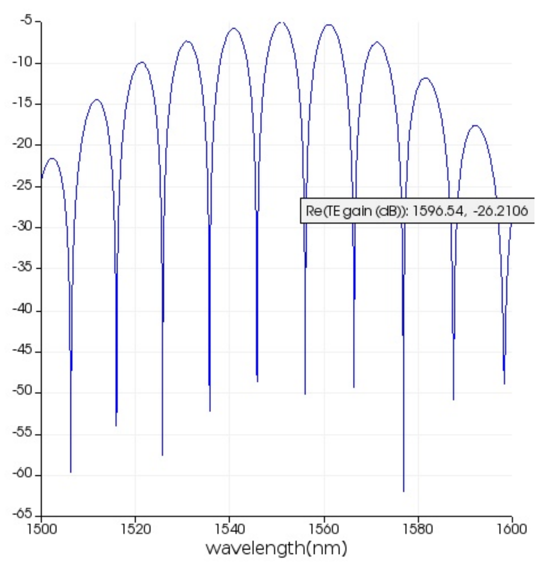

Fig. 3. Spectrum of first MZI with ΔL = 100μm.

4. Conclusion

This report described the main steps regarding different layout of MZIs, in the SOI technology, considering the waveguides in the strip configuration, with 220nm-height and 500nm-width.Initially untill now, three different geometries of MZI devices were designed for TE mode, using Lumerical, and Klayout for the mask drawing. The relation between the transmission spectrum over different wavelength from 1500 nm - 1600 nm was investigated with ΔL = 100 , 200, 300μm.

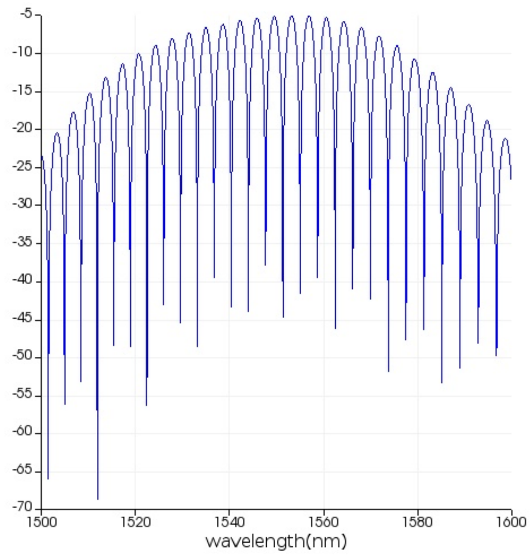

Fig. 4. Spectrum of first MZI with $\Delta L = 200\mu m$.

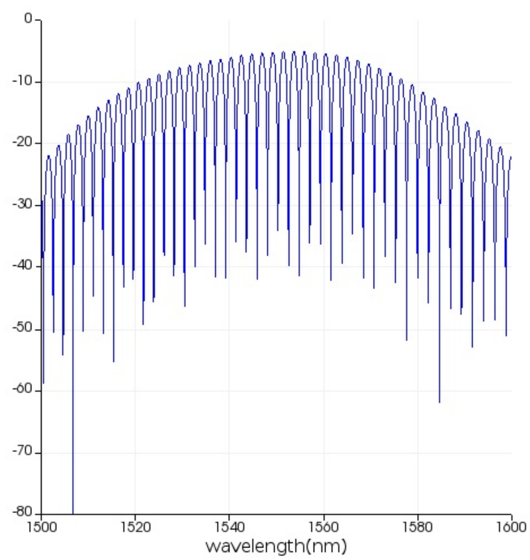

Fig. 5. Spectrum of first MZI with $\Delta L = 300\mu m$.

References

1. Subbaraman, H., Xu, X., Hosseini, A., Zhang, X., Zhang, Y., Kwong, D., & Chen, R. T., "Recent advances in silicon-based passive and active optical interconnects," Opt. Express **23**, 2487-2511 (2015).
2. K. Roberts et al, "High Capacity Transport100G and Beyond," J. Light. Technol. **vol.33, no.3**, 563-578 (2015).
3. Shoji, Y., Kintaka, K., Suda, S., Kawashima, H., Hasama, T., & Ishikawa, H., " Low-crosstalk 2× 2 thermo-optic switch with silicon wire waveguides," Opt. Express **18**, 9071-9075 (2010).
4. Li, T., Willner, A. E., & Kaminow, I., "Optical Fiber Telecommunications VA: Components and Subsystems," Acad. Press. (2010).
5. Chrostowski, L., & Hochberg, M., "Silicon photonics design: from devices to systems," Camb. Univ. Press.(2015).